Detection of the occupation of the costal diaphragmatic angle in chest radiographs

Luís A. Alexandre[1,2], Mário J. Silva[1,3], Aurélio C. Campilho[1,4]
[1] INEB - Instituto de Engenharia Biomédica,
[2] Departamento de Matemática/Informática, Universidade da Beira Interior,
E-mail: lfbaa@noe.ubi.pt,
[3] Centro Diagnóstico Pneumológico do Porto,
[4] Faculdade de Engenharia da Universidade do Porto,
E-mail: campilho@fe.up.pt

Abstract **– As part of a Computer-Aided Diagnosis system, a method to detect the occupancy of the costal diaphragmatic angles was developed. This paper presents the details of implementation and the results of tests on a chest radiographs database with 130 images. The results are good for the occupancy detection and not so good for the segmentation of the CDAs. Further developments are proposed.**

Resumo **– Foi desenvolvido um método de detecção de ocupação dos seios costo-diafragmáticos como parte dum sistema de auxílio ao diagnóstico. Este artigo apresenta os detalhes de implementação e os resultados de testes efectuados numa base de dados de 130 imagens de micro radiografias ao tórax. Os resultados são bons para a detecção de ocupação mas são mais fracos para a fase de segmentação dos seios costo-diafragmáticos. São propostos novos desenvolvimentos.**

Keywords **– Chest radiograph, costal diaphragmatic angle, computer-aided diagnosis**

Figure 1 - Normal radiograph showing both CDAs clear.

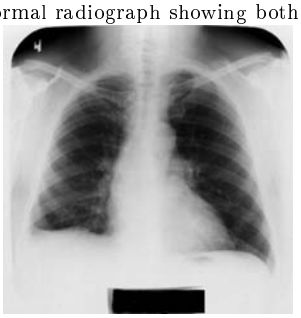

Figure 2 - Occupied right lung CDA.

I. Introduction

To facilitate the task of analysing chest radiographs, a Computer-Aided Diagnostic (CAD) system is under development at INEB. Since there is a variety of different pathologies that can be detected in a chest radiograph [1, 2, 3, 4, 5, 6], a divide-and-conquer approach is being used to tackle the problem. This means that for each pathology an appropriate method is being developed to detect its presence in the image.

This paper presents one of the methods developed. The goal is to detect whether the costal diaphragmatic angles (CDAs) are occupied.

This occupation can indicate an active or residual pathology. The most frequent in an active pathology is the pleural spill (presence of fluid between the pleura). This situation happens most frequently in the inflammatory and infectious processes, tuberculosis, cancer and cardiac insufficiency. As a residual process following these pathologies there is usually a tack between the pleura originating an occupancy of the costal diaphragmatic angles [2], [7].

This can be detected since in a normal lung the costal diaphragmatic angle ends in a sharp corner, otherwise it does not present such a corner. Figure 1 presents a normal radiograph where both CDAs present sharp corners, while figure 2 shows an image where the right CDA is occupied.

There are several difficulties in the analysis of these images. If the patient does not inhale properly, or the patient presents a large rib cage, the CDAs may not exhibit a sharp corner. Another problem occurs when the patient presents a large amount of fat tissue. An example of such a case is presented in figure 3. Breasts in women and large heart silhouettes, together with the presence of air in the stomach and in the colon, also interfere with the proper detection of the diaphragm (see figures 4 and 5).

The paper is organised as follows: in section II the

Figure 3 - Both CDAs are clear but difficult to detect due to a large amount of fat tissue.

Figure 4 - Left CDA difficult to detect due to large heart silhouette and the superposition of the breast.

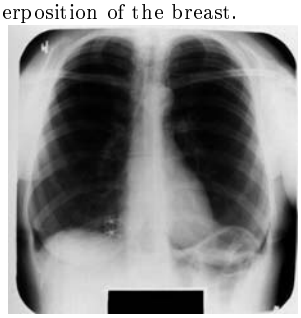

Figure 5 - Left CDA difficult to detect due to the presence of air in the colon and stomach and the superposition of the breast.

proposed method is described in detail. In section III the results of the experiments are presented and discussed. Finally, conclusions are posted in section IV.

II. Description

The images were digitised from a 10x10cm chest radiograph film to 2048x2048x12bit with a UMAX 1220S scanner. Some pre-processing was done. First, the greyscale depth was reduced to 8 bit. Then the images were sub-sampled to a size of 512x512.

The image analysis task is divided into several phases: 1) lateral lung edge delineation; 2) diaphragm line edge representation; 3) computing CDAs co-ordinates; 4) diaphragm slope characterisation close to the CDAs. These features were used as input to a multi-layer perceptron (MLP) to detect whether the CDAs were occupied.

A. Pre-processing

In order to reduce noise in the images and also to reduce the amount of information to process, without jeopardising the final goal, a reduction of the number of bits per pixel, from 12 to 8, and a resize of the images,

Figure 6 - Normal radiograph before the histogram stretch.

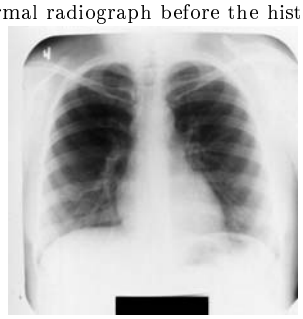

Figure 7 - Radiograph of figure 6 after the histogram stretch.

to 512x512, was done. The histogram was stretch so that the full 8 bit range was used by the images. The function used was:

$$IS = 255\frac{(I - min(I))}{(max(I) - min(I))}$$

where I is the original image and IS is the stretched image. The max and min functions return the highest and smallest gray value of the image, respectively. Figures 6 and 7 show an image before and after the histogram stretch. A different type of normalisation, based on the average levels of the lungs and mediastinum [8] was tested, but was not considered adequate to this problem.

B. Lung edge detection

We use a gradient plus thresholding approach to detect the external edge of the lungs [9]. Although it can produce well-defined objects, this technique can be difficult to automate. This happens because the result is critically dependent on filter size, and threshoding levels.

The detection of the exterior lung edges was done separately for the right and left lungs. We will describe the process for the right lung. The left lung exterior edge was obtained by the same process - differences will be referred when appropriate.

The first step was the definition of the region of interest (ROI). We find the vertical signature defined as,

$$VS(x) = \frac{1}{512}\sum_{k=1}^{512} IS(k, x).$$

Figure 8 shows a typical vertical signature. We find the maximum value of VS within the 1D ROI $x \in$

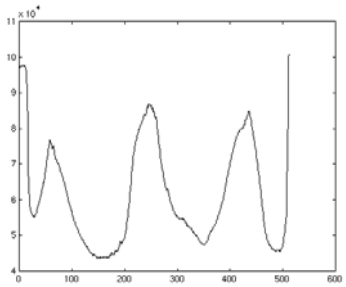

Figure 8 - Vertical signature for a typical image.

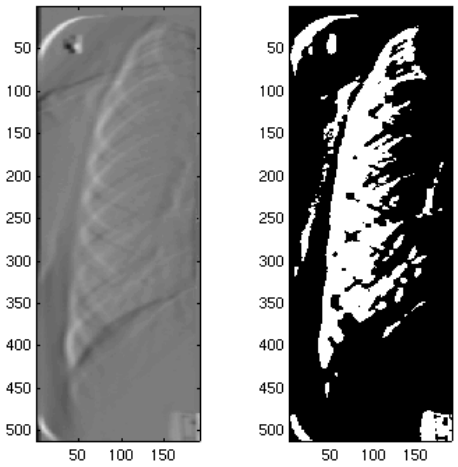

Figure 9 - First part of the process of finding the lateral lung edges: a) gradient of the ROI; b) thresholding at 127.

$512 * [0.4, 0.6]$ which we call MX. This point approximately coincides with the mediastinum. The right ROI is then defined as the subimage $IR(x, y) = IS(x, y)$, $x \in [20, MX-20]$, $y \in [1, 512]$. The left ROI is defined as $IL(x, y) = IS(x, y)$, $x \in [MX+20, 492]$, $y \in [1, 512]$. Note that a margin of 20 pixels was given at both ends of the ROIs. This avoids some noise present in the right and left portions of the image due to background fluctuations. It also gives a smaller margin for the area to process when we try to find the CDAs, since they are not found within a ± 20 pixels zone from MX.

Since the external edge of the lungs is approximately a vertical line, we applied a horizontal gradient filter to enhance vertical transitions. The result for one of the images is in figure 9a.

The resulting image was thresholded at 127 (figure 9b). This binarized image was again differentiated only in the horizontal direction, with a small window filter (figure 10a). This was again thresholded now at a level of 100.

Amongst the various lines we find the external edge of the lung. To isolate it we label all the objects in the image and build a new image containing only the largest object - this is the desired external lung edge. Finally, the edge was thinned. The result is presented in figure 10b. We are interested in finding de CDAs, consequently the only portion of the lung edges that we seek is the one that intercepts the diaphragm.

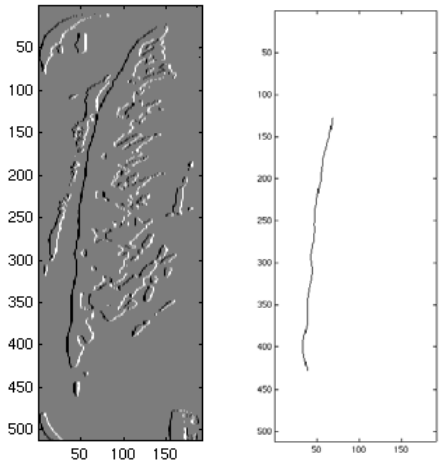

Figure 10 - Second part of the process of finding the lateral lung edges: a) horizontal gradient; b) egde after thresholding, selection and skeletonizing.

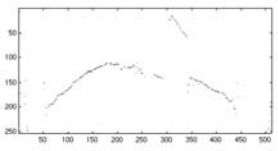

Figure 11 - Diaphragm detected.

C. Diaphragm detection

We start by defining a ROI. It is defined as the subimage $Ir(x, y) = IS(x, y)$, $x \in [1, 512]$, $y \in [205, 512]$. These limits were obtained empirically. What this ROI does is to exclude the top portion (40%) of the image from the processing, since we know the diaphragm is in the lower portion of the image.

Since the diaphragm is mainly a horizontal structure, the first operation is an approximation to a derivative in the vertical direction. Actually we did a convolution with a filter that detects vertical transitions from dark to bright regions. The resulting image was analysed leaving only the maximum value of the derivative for each column [10]. This can be justified since the diaphragm appears as the main transition from a dark to bright region that is oriented vertically. Problems could occur since the ribs can also fit in this description. To avoid them, the filter was constructed so that it only detects objects larger than the average rib. Figure 11 shows an example of a segmented diaphragm.

Note that this procedure does not obtain the diaphragm correctly in the zone were it is under the mediastinum. The reason is that in this zone the diaphragm is not a transition between a dark and a bright region. This is not important to us since we are only interested in the diaphragm near the CDAs. So we simply ignore the central part of the detected diaphragm.

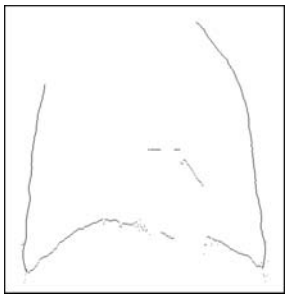

Figure 12 - Result of the segmentation of the CDAs.

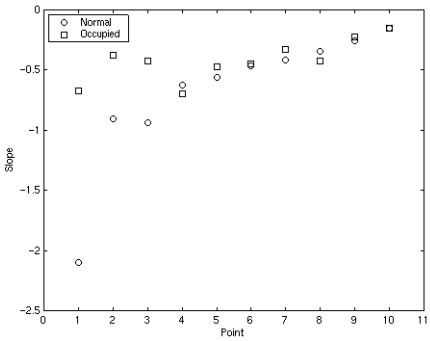

Figure 13 - Average slope of the right portion of the diaphragm.

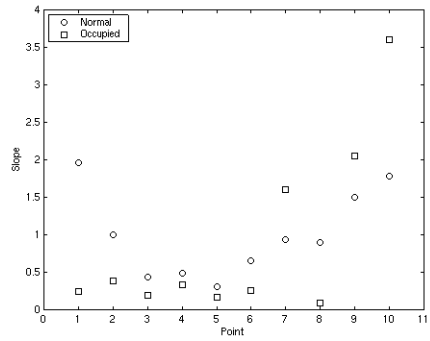

Figure 14 - Average slope of the left portion of the diaphragm.

D. Determining the occupancy of the CDAs

The intersection of the diaphragm with the lateral lung edges define the CDAs. Figure 12 shows this intersection for one image.

To decide if a CDA is occupied, we chose to analyse the region around the vertex of the CDAs and to compare the shape of the left and right portions of the diaphragm. In a normal image the portion of the diaphragm near the CDAs is almost symmetric. If one of the CDAs is occupied, that symmetry is lost. Also, the coordinates of the CDAs are important features since in a normal case, the vertex of the CDAs are approximately at the same height (eventually, in a normal patient, the right CDA may be in a lower position than the left).

The decision as to the occupancy of the CDAs is made by a multi-layer perceptron (MLP). It has two outputs: one for each CDA. A value of 0 means a clear CDA and a value of 1 means an occupied CDA. One of features used is obtained from the coordinates of the vertices of the CDAs. Since the important coordinate is the height, we do not use the X coordinate. And also the important thing is the relative position of the vertices, so we only use the difference between the heights of the vertices.

To analyse the shape of the diaphragm near the CDAs, we compute the slope of the diaphragm in 10 equally distant points for each CDA. The values of the slopes for the right and left CDAs, in a normal radiograph, are almost symmetric. In the case of an occupied CDA, this symmetry is lost. To calculate these slopes, the difference in height between each two consecutive points was divided by their spacing. Note that the points are all equally spaced. Figures 13 and 14 show the average slope of the right and left portion of the diaphragm respectively, for the 130 images used in the classification step. Each figure presents the average value for both the normal and occupied CDAs.

Notice how the slope near the CDA (first points) is smaller (in absolute value) for the pathologic images: this is a clear evidence of the occupation of the CDA. Also, the right slopes appear as negative values and the left as positive due to the fact that we use the origin of the axis in the top left corner of the images. The last points in figure 14 appear with high values for the slope since they represent the slope on the heart's shadow region.

We could use as features to the MLP only the differences between each pair of corresponding right/left slopes. Since a symmetry would yield values close to zero, an asymmetry would yield high values. But this would fail to detect the cases where both CDA are occupied: in this case there would also be a symmetry between the CDAs. What distinguishes these cases from a normal one is the shape of the CDAs. So, as features, we used the two sets of 10 values of the slopes of the diaphragm near the CDAs and the difference between the heights of the vertices of the CDAs. This means that the MLP has 2 x 10 + 1 = 21 features as inputs. Its topology is 10 x 12 x 2 : 10 neurons in the input layer, 12 in the hidden layer and 2 in the output layer. This topology was obtained empirically, after several tests.

III. Experiments

A database of 174 images was build. From this initial set, 44 were eliminated because they were not technically correct: women did not remove their bras or the lungs were not completely in the image. Even so we kept some images that are not technically correct since they are over or underexposed. The database used for the experiments was then constituted by 130 images. Of these, 16 images present one occupied CDA (11 left CDA and 5 right CDA). We consider two parts in the experiment: the first consists in the correct detection of the diaphragm and external lung edges, allowing the correct identification of the CDAs' coordinates

(segmentation). The second part is the detection of the occupancy of the CDA given already correctly segmented images (classification). Note that the case of both occupied CDAs was not used since it is not represented in the database.

A. Segmentation

The algorithms were applied to the 130 images in the database. The segmentation results are presented in table I.

Right CDA	*Left CDA*
15.0%	26.7%

Table I

Percentage of error in the segmentation.

The evaluation of the segmentation performance was done considering a correct segmentation of the CDA if the external lung edge intercepted the diaphragm in the correct location and the diaphragm was correctly segmented in the zone of the CDA. The experiments show that the diaphragm is almost always correctly detected - even when there are problems, the portion close to the vertex of the CDA is detected. The main problems are large heart silhouette and air in the colon and stomach, and these affect only the left CDA. The detection of the lateral lung edges has some problems: sometimes they are not completely detected. And even if they are detected an intersection with the diaphragm may not occur, which prevents the CDAs from being defined. When these cases occurred we completed manually the lung edge in order to be possible to define the CDA, so that all 130 images were available to the occupancy detection algorithm.

B. Classification

The MLP was trained with resilient backpropagation [11], using a set composed of 129 samples, and its performance was tested on the remaining sample (leave-one-out cross-validation method [12]). This was done for all 130 samples. Each time the network was trained for 250 epochs. The features were pre-processed in order to have zero mean and unit variance. They were also orthogonalized using principal component analysis. The experience was repeated 50 times and the resulting average confusion matrixes are presented in tables II and III with the respective standard deviation.

There is an average error of 7.28% in the classification of the right CDA (given by the average 9.46 misclassified cases in a total of 130) and an average error of 7.26% in the classification of the left CDA (given by the average 9.44 misclassified cases in a total of 130). The fact that the error for the left CDA is inferior to the error for the right CDA was not expected since, as mentioned before, there are several facts that affect the correct segmentation of the left portion of the diaphragm. A probable explanation for this fact lies

Right CDA		Assigned Class	
		Clear	*Occupied*
Actual Class	*Clear*	93.98(1.58)	6.02(1.52)
	Occupied	38.80(15.40)	61.20(15.40)

Table II

Average confusion matrix for the right CDA occupancy.

Left CDA		Assigned Class	
		Clear	*Occupied*
Actual Class	*Clear*	93.98(1.65)	6.02(1.65)
	Occupied	20.73(5.55)	79.27(5.55)

Table III

Average confusion matrix for the left CDA occupancy.

in the existence of more samples of left CDAs with pathology that right CDAs (11 and 5, respectively). This may enable a better approximation by the MLP to the left than the right pathologic CDA, compensating for the probable less accurate segmentation of the left CDA.

There are two types of errors that this system can make: a false negative (an occupied CDA that is not detected) and a false positive (a clear CDA that is reported as being occupied). Of these, the first is the most dangerous since it allows a pathologic case to go unnoticed. In these experiments we see that the percentage of false negatives is 38.8% and 20.7% for the right and left CDAs, respectively. Again, better results are presented by the left CDA and we use the same justification as above: since there are more samples of left occupied CDAs these are better approximated by the MLP than the right occupied CDAs. In any case, these percentages are rather high and should be reduced. We believe that with more pathologic cases the MLP would show a better performance for this particular case. Another solution to this problem is discussed in the conclusions.

IV. Conclusions

A method to detect the occupancy of the costal diaphragmatic angle was developed. It is based on the computerized analysis of digitalized chest radiographs.

The results obtained indicate that the method for deciding if the CDAs are occupied, once the correct segmentation has occurred is reasonable (7.3% error for both CDAs). The CDAs' segmentation is not yet optimised since the detection of the lung edges needs to be improved (20.9% average error). The results obtained so far are promising, however more abnormal cases are needed in order to reduce the amount of false positives.

We note that this is not an easy problem given the high variability of shapes among different people and the relatively small differences we are studying: the diaphragm shape is dependent on several factors already mentioned and sometimes a normal diaphragm of a given person may be closer to the average pathologic

diaphragm than to the average normal diaphragm.

A. Future developments

We are considering an alteration to the classification process to reduce the false negatives based in the certainty of the classifier in its classification: if the classifier is not 'almost shure' about the CDA being free than it must be considered occupied. This implies the introduction of measures of confidence of the classifier on its decisions. This will reduce the false negatives at the expense of the false positives, which will increase.

We are also considering an extension of this work that is able to distinguish between an occupation of the CDA due to the presence of fluid or the occupation due to a pleural tack.

References

[1] S.M. Lai, X. Li, and W.F. Bischof, "Automated detection of breast tumors", in *Computer Vision and Shape Recognition*, A. Krzyzak, T. Kasvand, and C.Y: Suen, Eds. 1989, pp. 115–132, World Scientific.

[2] I.B. Pena, *Radiolagia clinica del torax*, Ediciones Toray, S.A., Barcelona, 1970.

[3] M.J. Carreira, D. Cabello, M.G. Penedo, and A. Mosquera, "Computer-aided diagnoses: Automatic detection of lung nodules", *Med. Phys.*, vol. 25, no. 10, pp. 1998–2006, October 1998.

[4] M.G. Penedo, M.J. Carreira, A. Mosquera, and D. Cabello, "Computer-aided diagnosis: A neural-network based approach to lung nodule detection", *IEEE Trans. Medical Imaging*, vol. 17, no. 6, pp. 872–880, December 1998.

[5] X. Xu, K. Doi, T. Kobayashi, H. MacMahon, and M.L. Giger, "Development of an improved CAD scheme for automated detection of lung nodules in digital chest images", *Med. Phys.*, vol. 24, no. 9, pp. 1395–1403, September 1997.

[6] H. Yoshida, S. Katsuragawa, Y. Amit, and K. Doi, "Wavelet snake for classification of nodules and false positives in digital chest radiographs", in *19th International Conference IEEE/EMBS*, Chicago,IL,USA, 1997, pp. 509–512.

[7] C.S. Pedrosa and R. Casanova, *Diagnostico por imagen*, Interamericana - McGraw-Hill, 1987.

[8] O. Tsujii, M.T. Freedmann, and S.K. Mun, "Automated segmentation of anatomic regions in chest radiographs using an adaptive-sized hybrid neural network", *Med. Phys.*, vol. 25, no. 6, pp. 998–1007, June 1998.

[9] A.K. Jain, *Fundamentals of Digital Image Processing*, Prentice-Hall, 1987.

[10] B. van Ginneken and B.M.H. Romeny, "Automatic segmentation of lung fields in chest radiographs", 1999, Accepted for MICCAI'99 - http://neuromedia.ukc.ac.uk/miccai99/.

[11] H. Demuth and M. Beale, *Neural Network Toolbox User's Guide*, The MathWorks, Inc., 1998.

[12] F. Blayo, Y. Cheneval, A. Guérin-Dugué, C. Chentouf, C. Aviles-Cruz, J. Madrenas, M. Moreno, and J.L. Voz, "Deliverable R3-B4-P - Task B4:benchmarks", Tech. Rep. 6891, ESPRIT-Basic Research Project, June 1995.